Therapeutic Effect of Imatinib in Gastrointestinal Stromal Tumors: AKT Signaling Dependent and Independent Mechanisms

Chi Tarn,[1] Yuliya V. Skorobogatko,[1] Takahiro Taguchi,[2] Burton Eisenberg,[3] Margaret von Mehren,[1] and Andrew K. Godwin[1]

[1]Department of Medical Oncology, Fox Chase Cancer Center, Philadelphia, Pennsylvania; [2]Department of Neurobiology and Anatomy, Kochi Medical School, Nankoku, Japan; and [3]Norris Cotton Cancer Center, Dartmouth-Hitchcock Medical Center, Lebanon, New Hampshire

Abstract

Most gastrointestinal stromal tumors (GISTs) possess a gain-of-function mutation in *c-KIT*. Imatinib mesylate, a small-molecule inhibitor against several receptor tyrosine kinases, including KIT, platelet-derived growth factor receptor-α, and BCR-ABL, has therapeutic benefit for GISTs both via KIT and via unknown mechanisms. Clinical evidence suggests that a potential therapeutic benefit of imatinib might result from decreased glucose uptake as measured by positron emission tomography using 18-fluoro-2-deoxy-D-glucose. We sought to determine the mechanism of and correlation to altered metabolism and cell survival in response to imatinib. Glucose uptake, cell viability, and apoptosis in GIST cells were measured following imatinib treatment. Lentivirus constructs were used to stably express constitutively active AKT1 or AKT2 in GIST cells to study the role of AKT signaling in metabolism and cell survival. Immunoblots and immunofluorescent staining were used to determine the levels of plasma membrane-bound glucose transporter Glut4. We show that oncogenic activation of KIT maximizes glucose uptake in an AKT-dependent manner. Imatinib treatment markedly reduces glucose uptake via decreased levels of plasma membrane-bound Glut4 and induces apoptosis or growth arrest by inhibiting KIT activity. Importantly, expression of constitutively active AKT1 or AKT2 does not rescue cells from the imatinib-mediated apoptosis although glucose uptake was not blocked, suggesting that the potential therapeutic effect of imatinib is independent of AKT activity and glucose deprivation. Overall, these findings contribute to a clearer understanding of the molecular mechanisms involved in the therapeutic benefit of imatinib in GIST and suggest that a drug-mediated decrease in tumor metabolism observed clinically may not entirely reflect therapeutic efficacy of treatment. (Cancer Res 2006; 66(10): 5477-86)

Introduction

Gastrointestinal stromal tumors (GISTs) are the most common mesenchymal tumors of the digestive tract. GIST cells are believed to emanate from a progenitor of the interstitial cells of Cajal (1, 2), a population of spindle cells that are pacemaker cells of the gut, or from an interstitial mesenchymal precursor stem cell (3). Most GISTs express gain-of-function mutations of KIT, the receptor tyrosine kinase (RTK) encoded by the *c-KIT* proto-oncogene (4, 5). It has also been noted that ~10% GIST are wild-type for *c-KIT*, with 30% of these harboring activating mutations in the platelet-derived growth factor receptor (PDGFR) α (6).

KIT, a 145-kDa transmembrane glycoprotein, is a member of the RTK type III family that includes PDGFR, macrophage colony-stimulating factor receptor, and FMS-like tyrosine kinase 3 (7–10). These receptor kinases share common structural features: an extracellular domain made up of five immunoglobulin-like repeats, a strongly conserved juxtamembrane domain, and a tyrosine kinase domain that is split into two domains by an insertion sequence of variable length (11).

KIT oncogenic activation results in autophosphorylation of tyrosine residues, which serve as docking sites for various signaling intermediates (12, 13). KIT signaling regulates mechanisms that are crucial for differentiation, phosphorylation, apoptosis, neoplastic transformation, and malignant progression (14–17). However, KIT signals have variable biological effects depending on the cellular context. Therefore, the signaling pathway data in various normal and cancer cell models do not predict which KIT signaling pathways are critical for oncogenic behavior in GIST. It has been shown that, depending on the KIT mutation, various KIT oncoproteins differ in their structure and activation of specific downstream signaling pathways (8, 18).

Clinical trials have found that GISTs are sensitive to imatinib mesylate (Gleevec, STI571, Novartis, Basel, Switzerland), which acts as a selective inhibitor for the KIT, PDGFR, and BCR-ABL tyrosine kinases (19–22). *In vitro,* imatinib mesylate rapidly inhibits KIT phosphorylation and tumor cell proliferation in GIST cell lines (23, 24). Clinically, imatinib mesylate has been successfully tested in clinical trials of GIST patients with metastatic and/or unresectable tumors (25–27).

Cancer cells use glucose abnormally when compared with normal, nontransformed cells (28). The accelerated rate of glucose uptake and metabolism in tumor cells is multifactorial and may occur as a consequence of oncogenic transformation (29, 30). Glucose uptake by tumors can be clinically detected by positron emission tomography (PET) scan using 18-fluoro-2-deoxy-D-glucose (FDG). In GIST, FDG inhibition is a sensitive method to evaluate early response to imatinib treatment (27, 31). In chronic myelogenous leukemia (CML), imatinib mesylate inhibits the oncogenic activity of the tyrosine kinase BCR-ABL (32) and decreases glucose uptake from the medium by BCR-ABL-positive cells (33). Given the above clinical and experimental observations (i.e., that imatinib mesylate decreases glucose uptake by GIST *in vivo* as observed by PET scanning and in CML cell lines *in vitro* and that imatinib mesylate is an inhibitor of specific tyrosine kinases), we decided to evaluate the changes in glucose uptake in

Note: Supplementary data for this article are available at Cancer Research Online (http://cancerres.aacrjournals.org/).

Requests for reprints: Andrew K. Godwin, Department of Medical Oncology, Fox Chase Cancer Center, 333 Cottman Avenue, Philadelphia, PA 19111. Phone: 215-728-2205; Fax: 215-728-2741; E-mail: Andrew.Godwin@fccc.edu.

doi:10.1158/0008-5472.CAN-05-3906

response to imatinib in GIST. The purpose of our study was to determine the association of altered glucose uptake directly with cell survival as an indicator of therapeutic benefit of imatinib mesylate and to determine the molecular mechanisms that regulate the alteration of glucose uptake and GIST cell survival.

We report that constitutively active KIT is associated with a high rate of glucose uptake in GIST cells. Imatinib mesylate inhibits KIT activity and leads to down-regulation of AKT, resulting in decreased glucose uptake by the tumor cells. We further show that endocytosis of the Glut4 transporter from the cell surface leads to decreased glucose uptake due to inhibition of AKT activity with imatinib mesylate. However, imatinib mesylate–induced cell growth arrest and eventual apoptosis are independent of AKT activity and may therefore be independent of glucose uptake. Most importantly, we show that activation of the AKT pathway, although acknowledged as a survival pathway that is notably down-regulated by imatinib mesylate, is not the mechanism of GIST cell survival. Additionally, this work suggests that decrease in glucose uptake by GIST cells after imatinib mesylate may not be the only mechanism that results in cell death. In summary, we have shown that tumor growth inhibition and induction of apoptosis by imatinib mesylate is not singularly dependent on changes in glucose uptake or on the inhibition of the AKT signaling pathway.

Materials and Methods

Chemicals. Imatinib mesylate (Gleevec, STI571, obtained from the Fox Chase Cancer Center pharmacy, Philadelphia, PA) was dissolved in sterile PBS and stored at −20°C. 2-^{3}H-deoxy-glucose was purchased from Amersham Biosciences (Piscataway, NJ). LY294002 and U0126 were purchased from Calbiochem (La Jolla, CA). All antibodies (except β-actin, anti-Glut1, Glut4, and Na/K ATPase-α1) used in this study were purchased from Cell Signaling Technologies (Beverly, MA) and used according to the manufacturer's instruction. Anti-β-actin antibody was purchased from Sigma (St. Louis, MO). Anti-Glut4 antiserum used in immunostaining was a generous gift from Dr. Morris Birnbaum (University of Pennsylvania, Philadelphia, PA). Anti-Glut4 and anti-Glut1 antibodies used for immunoblots were purchased from Abcam (Cambridge, MA). Anti-Na/K ATPase-α1 antibody was purchased from Novus Biologicals (Littleton, CO). Horseradish peroxidase (HRP)–conjugated secondary antibodies were purchased from Amersham Biosciences. Fluorophore-conjugated secondary antibodies and Vybrant cell-labeling solutions for membrane labeling were purchased from Molecular Probes (Eugene, OR).

Cell cultures. GIST 882 cells, a generous gift from Dr. Jonathon Fletcher (Brigham and Women's Hospital, Boston, MA), possess a homozygous mutation in c-*KIT* exon 13 and were grown as described previously (24). GIST T1 cells (34) possess a homozygous mutation in c-*KIT* exon 11 and were maintained in DMEM supplemented with 10% fetal bovine serum and glutamine. For imatinib treatment, imatinib was added directly to the cell medium at a final concentration indicated in each result.

Preparation of whole-cell extract from cells and immunoblot assays. The whole-cell extract was prepared as described previously (24). Whole-cell extract (50 μg) was electrophoresed and blotted onto Immobilon-P membrane (Millipore, Billerica, MA). Membranes were incubated with primary antibodies (1:1,000 dilution for all primary antibodies used in this study) and diluted in TBS/0.5% Tween 20 with 5% bovine serum albumin (BSA) at 4°C overnight followed by HRP-conjugated secondary antibody at room temperature for 1 hour. Protein bands were detected by Western Lighting Plus chemiluminescence reagent (Roche, Indianapolis, IN).

Viability and apoptosis assays. GIST cells were seeded at 4×10^5 per six-well plates and treated with drugs for indicated time points. For cell growth and viability assays, cells were harvested by trypsinization at each time point, washed in PBS, and stained using Guava ViaCount Reagent (Guava Technologies, Inc., Hayward, CA). The IC_{50} was determined by treating cells with varying doses of drugs for 72 hours, and the value of IC_{50} was determined at the concentration when there was a 50% reduction in cell number. For apoptosis assays, cells were harvested at 72 hours after treatment and stained using the Guava Nexin kit according to manufacturer's recommendations. Cell populations were analyzed by the Guava Personal Cell Analysis system, and data were processed using CytoSoft software (Guava Technologies).

Glucose uptake assay. GIST cells were seeded at 5×10^5 per six-well plate. After treatment, cells were rinsed twice with prewarmed glucose uptake buffer [118 mmol/L NaCl, 5 mmol/L KCl, 1.3 mmol/L $CaCl_2$, 1.2 mmol/L $MgSO_4$, 1.2 mmol/L KH_2PO_4 (pH 7.4)]. After rinsing, 500 μL prewarmed glucose uptake buffer was added to each well, and the cells were incubated at 37°C for 10 minutes. 10× uptake buffer (50 μL; 1 mL glucose uptake buffer contains 5 μCi 2-^{3}H-deoxy-glucose and 50 μmol/L glucose) was then added to each well followed by incubation of cells at 37°C for an additional 10 minutes. The uptake was terminated by washing the cells five times with PBS followed by lysis with 500 μL of 0.1% SDS at room temperature for at least 30 minutes. Cell lysates were transferred into scintillation vials, and each well was rinsed with additional 500 μL distilled water. Then, the total volume was collected and subjected to protein quantitation and scintillation counting. Cytochalasin B (10 μmol/L; Sigma) was used as background control for glucose uptake and subtracted from all counts. To determine the percentage (%) of glucose uptake, uptake per minute per mg protein (cpm/min/mg) was calculated based on cpm and total protein concentration. The absolute uptake was then normalized with nontreated samples to determine the percentage of uptake. At least three independent uptake assays were done for each experiment, and experimental variations and significance were determined by SD.

Lentiviral construction. Myristoylated human AKT1 coding region was amplified by reverse transcription-PCR using forward (5′-ATACTCTAGAGCCACCATGGGGAGCAGCAAGAGCAAGCCCAAGGACCCCAGCCAGCGCCGGAGCGACGTGGCTATTGTGAAG-3′), which contains both the Kozac and myristoylation sequences (35), and reverse (5′-ATACGGATCCTCAGGCATAATCGGGTACATCGTAAGGGTAGGCCGTGCTGCTGGCCGAGT-3′) primers, in which a stop codon was incorporated. Total RNA template was isolated from GIST T1 cells using Trizol reagent following the manufacturer's instruction (Invitrogen, Carlsbad, CA). cDNA was synthesized using avian myeloblastosis virus reverse transcriptase (Promega, Madison, WI). The PCR was carried out following the manufacturer's instruction using Expand High Fidelity PCR System (Roche). The PCR product was then cloned in pCR2.1-TOPO vector (Invitrogen), and the DNA sequence was verified and subcloned into pENTR3C vector (ViraPower Lentiviral Expression system, Invitrogen). The myristylated human AKT2 construct in DsRed2 vector was kindly provided by Dr. Jin Cheng (Moffitt Cancer Center, University of South Florida, Tampa, FL) and subcloned into pENTR3C vector. Amphotropic T293FT cells were used to generate viral stock following the manufacturer's instruction (ViraPower Lentiviral Expression system). Lentivirus expressing myristylated AKT1 or AKT2 was used to infect GIST T1 cells generating GIST T1/AKT1 and GIST T1/AKT2 cell lines, respectively. Lentiviral vector expressing *LacZ* gene as control was provided by the manufacturer.

Immunostaining and microscopy. Cells were fixed with 4% paraformaldehyde for 20 minutes at room temperature followed by extensive washing with PBS to remove excess paraformaldehyde. Cells were then permeabilized with PBS containing 0.2% Triton X-100 for 5 minutes at room temperature followed by three PBS washes with gentle shaking. Permeabilized cells were blocked in PBS plus 1% BSA for 1 hour at room temperature. The cells were then incubated with primary antibodies (1:200 dilution for anti-phosphorylated AKT Ser^{473} antibody and 1:100 dilution for anti-Glut4 antibody) for 1 hour at 37°C. Cells were washed thrice with PBS and then incubated with Alexa Fluor–labeled secondary antibodies (Alexa Fluor 448 for green fluorescence and Alexa Fluor 647 for far-red fluorescence; Molecular Probes) for 1 hour at room temperature. To counterstain nuclei, cells were washed with PBS containing 1 μg/mL propidium iodide for 15 minutes at room temperature. Images were acquired using Nikon (Tokyo, Japan) E800 upright microscope with a Bio-Rad (Hercules, CA) Radiance 2000 confocal scanhead facilitated with

LaserSharp2000 software for acquisition. The images were acquired sequentially to avoid emission bleed-through.

Subcellular fractionation and sucrose gradient centrifugation. GIST cells were maintained in growth medium with and without imatinib treatment for 40 hours. After incubation, cells were washed twice with PBS, scraped, and pelleted by centrifugation at 1,500 rpm for 5 minutes. The cell pellets were resuspended in HES buffer [20 mmol/L HEPES (pH 7.4), 1 mmol/L EDTA, 250 mmol/L sucrose] supplemented with protease inhibitor cocktail (Roche) and 250 nmol/L phenylmethylsulfonyl fluoride (Sigma). The cells were homogenized by passing through a 31-gauge needle six times. Nuclei, mitochondria, and plasma membrane were obtained by centrifugation at 14,000 × *g* for 15 minutes (Sorvall Super T21). The resulting pellet was resuspended in 5 mL HES buffer and layered on 5 mL of 1.12 mol/L sucrose cushion [20 mmol/L HEPES (pH 7.4), 1 mmol/L EDTA, 1.12 mol/L sucrose] and centrifuged at 100,000 × *g* in a SW41 rotor (Beckman, Fullerton, CA) for 1 hour at 4°C. The white, fluffy, middle layer is the plasma membrane containing fraction. The plasma membrane fraction was then resuspended with 10 mL HES and pelleted by centrifugation at 40,000 × *g* in a SW41 rotor for 20 minutes at 4°C. The protein concentration of plasma membrane fraction was determined according to Bradford methods. Protein (10 μg) from the plasma membrane fraction was subjected to immunoblotting assays as described previously.

Results

Sensitivity of GIST cells to imatinib as a function of c-*KIT* mutational status. Recent clinical studies have shown that response to imatinib mesylate in GIST patients is dependent on the mutational status of KIT (36). Using *in vitro* model systems, we evaluated two GIST cell lines, GIST 882 and GIST T1, for their sensitivity to imatinib. GIST 882 cells possess a missense mutation in exon 13 (K642E), whereas GIST T1 cells contain a 57-nucleotide in-frame deletion in exon 11 (V560_Y579del). Our results showed that imatinib mesylate blocks autophosphorylation of KIT in both GIST 882 and GIST T1 cells but at different drug concentrations. Imatinib mesylate at 0.01 μmol/L concentration significantly inhibits KIT autophosphorylation in GIST 882 cells, whereas GIST T1 cells required treatment with 0.1 μmol/L imatinib mesylate to completely block KIT autophosphorylation (Fig. 1*A*). Intriguingly, imatinib mesylate concentrations required for the inhibition of KIT phosphorylation did not correlate well with cell viability and growth of GIST cells (Fig. 1*B*; data not shown). We determined that GIST T1 cells were ~30-fold more sensitive to imatinib mesylate than GIST 882 cells with regard to cell growth. The IC_{50} (50% reduction in cell number) was ~25 nmol/L imatinib mesylate for GIST T1 cells versus ~750 nmol/L imatinib mesylate for GIST 882 cells as determined by evaluating cell number at varying doses of imatinib mesylate (0-10 μmol/L; data not shown). Next, we showed that exposure to imatinib mesylate effectively induced apoptosis in GIST T1 cells but not in GIST 882 cells as determined by fluorescence-activated cell sorting analysis using Annexin V and 7-aminoactinomycin staining (Fig. 1*C*). GIST 882 cells treated with imatinib mesylate show no significant increase in either early or late apoptosis during the 72-hour treatment period. In comparison, we observed a 3- to 5-fold increase in apoptotic cells in GIST T1 (Fig. 1*C*). These results suggest that V560_Y579del mutant KIT is particularly sensitive to imatinib mesylate–induced cell death by clinically relevant concentrations of imatinib mesylate compared with cells with the missense mutation in exon 13 (K642E), supporting findings in clinical studies (37, 38), and that the phosphorylation status of KIT alone was not reflective of biological response to imatinib mesylate.

Imatinib treatment causes dephosphorylation of KIT and AKT and decreases glucose uptake in GIST cells. We next

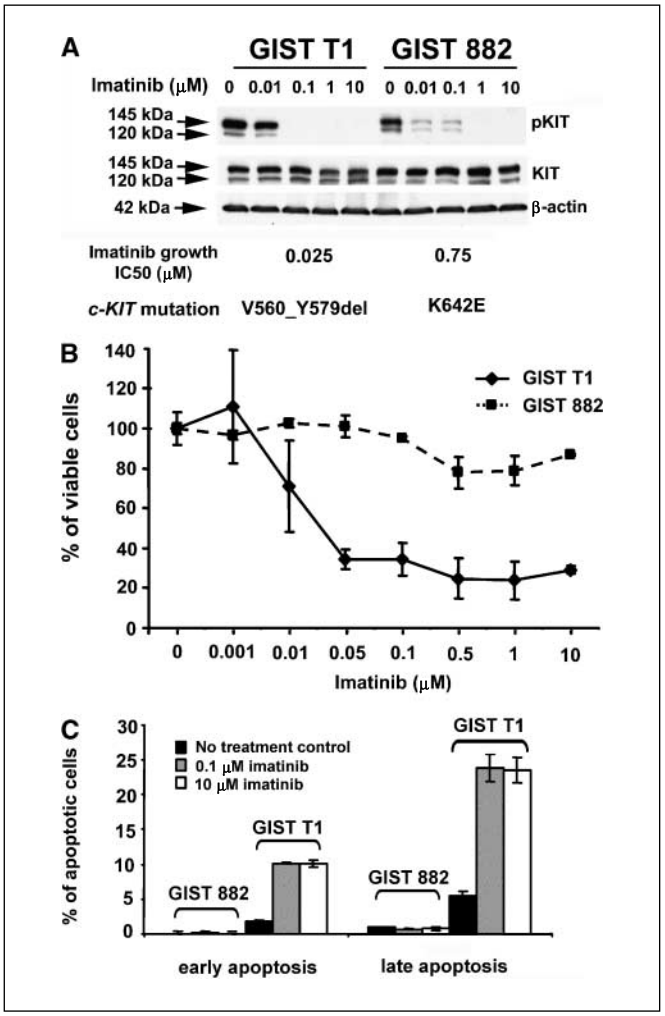

Figure 1. Differential responses of GIST cell lines to imatinib treatment. *A,* immunoblot assays of GIST T1 and GIST 882 cells treated with imatinib mesylate for 6 hours at indicated concentrations. Equal amounts of whole-cell extract from each sample were subjected to immunoblot assays using specific anti-phosphorylated KIT and KIT antibodies. The mutational status of GIST T1 and GIST 882 cells are indicated below each figure. *B,* cell viability assays. GIST T1 and GIST 882 cells were treated at various concentrations of imatinib mesylate for 72 hours. Percentage of cell viability was derived by normalizing the number of viable cells in the treated samples to that of nontreated samples. *Points,* statistical summary of three independent experiments. *C,* apoptosis assays. GIST T1 and GIST 882 cells were treated with imatinib mesylate at the indicated concentration for 72 hours. Percentage of apoptotic cells were derived by dividing the number of apoptotic cells with the number of total cells.

examined the phosphorylation status of purported downstream mediators of KIT signaling [e.g., AKT and mitogen-activated protein kinase (MAPK1/MAPK2)] after imatinib mesylate treatment. As shown in Fig. 2, imatinib mesylate strongly inhibited phosphorylation of KIT in both cell lines beginning as early as 1 hour and persisted for at least 24 hours (Fig. 2*A* and *B*). Treatment with LY 294002 (Fig. 2*A* and *B, lane LY*) and U0126 (Fig. 2*A* and *B, lane U*), the specific inhibitors of phosphatidylinositol 3-kinase (PI3K) and MAPK/extracellular signal-regulated kinase kinase (MEK1/MEK2), respectively, did not cause dephosphorylation of KIT, confirming that KIT dephosphorylation is imatinib mesylate specific. In addition, imatinib mesylate caused a decrease in phosphorylated AKT at Ser^{473} and Thr^{308} residues. Treatment with LY294002 did not alter the phosphorylation status of KIT, although it caused

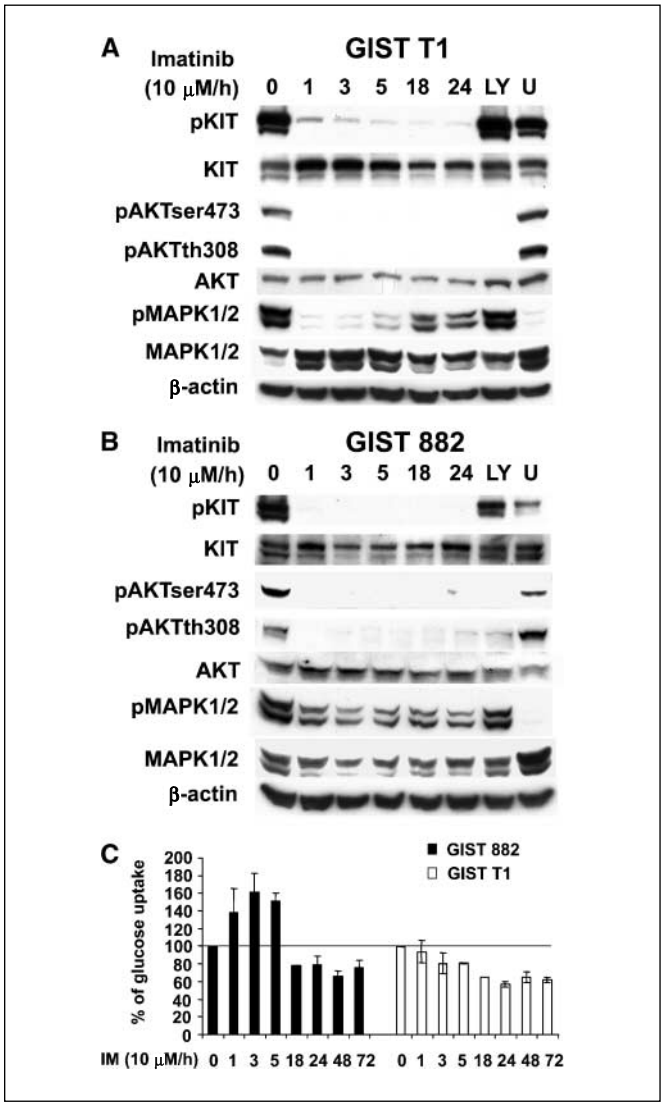

Figure 2. Imatinib treatment results in dephosphorylation of KIT and AKT and decreased glucose uptake in GIST cells. GIST T1 (*A*) and GIST 882 (*B*) cells were treated with 10 μmol/L imatinib mesylate for the indicated time points. Equal amounts of whole-cell extract from each sample were subjected to immunoblotting using specific antibodies as indicated. *Lanes LY* and *U,* cells were treated with 30 μmol/L LY294002 and 10 μmol/L U0126, respectively. *C,* glucose uptake assays of GIST 882 and GIST T1 cells treated with imatinib mesylate for the indicated time points. The percentage of uptake was normalized to nontreated samples (0 hour). *Columns,* statistical summary of four independent experiments.

dephosphorylation of AKT (Fig. 2*A* and *B, lane LY*). This result indicates that AKT is a shared downstream effector of both KIT and PI3K activity in GIST. In GIST T1 cells, imatinib mesylate leads to a transient dephosphorylation of MAPK1/MAPK2 (Fig. 2*A*). Interestingly, the phosphorylation of MAPK1/MAPK2 recovered over time during imatinib mesylate treatment. This phenomenon could be secondary to activation of another signaling pathway leading to phosphorylation of MAPK1/MAPK2 when KIT-AKT signaling is inhibited. However, in GIST 882 cells, imatinib mesylate inhibits phosphorylation of MAPK1/MAPK2 throughout the observed time course. These data agree with the clinical observations that KIT mutation status of GIST determines response to imatinib mesylate therapy. For all conditions tested, the total levels of KIT, AKT, and MAPK1/MAPK2 remained unchanged throughout treatments.

Published data indicate that FDG-PET is an early and sensitive method to evaluate response to imatinib mesylate treatment (19, 27, 39). Using FDG, we determined that imatinib mesylate directly reduces glucose transport into GIST cells in culture. GIST T1 displayed an imatinib mesylate–dependent decrease in glucose uptake as a function of time, whereas GIST 882 cells showed an initial increase in glucose uptake for up to 5 hours after addition of imatinib mesylate followed by a sharp decrease of glucose uptake (Fig. 2*C*). This result clearly shows that imatinib mesylate treatment directly leads to decreased glucose transport into GIST cells *in vitro* similar to what is seen by clinical FDG-PET. It is important to note that activating KIT maximizes AKT phosphorylation and glucose uptake in GIST cell. However, the addition of insulin does not have a synergistic effect on KIT-mediated glucose uptake, although the insulin receptor is expressed in both GIST cell lines (data not shown).

LY294002 treatment causes dephosphorylation of AKT and decreases glucose uptake in GIST cells. To further determine the mechanism by which imatinib mesylate treatment decreases glucose uptake, LY294002, a specific inhibitor of PI3K, was used to examine the role of AKT in glucose uptake. AKT is the major target for PI3K, and inhibition of PI3K directly leads to inactivation of AKTs. Previously, we have shown that LY294002 effectively caused dephosphorylation of AKT at both Ser^{473} and Thr^{308} residues in GIST 882 cells (24). In this study, we examined the inhibitory effect of LY294002 on GIST T1 cells in comparison with GIST 882 cells. LY294002 treatment caused strong dephosphorylation of AKT at both Ser^{473} and Thr^{308} residues as early as 1 hour after treatment and lasted for at least 24 hours (Fig. 3*A* and *B*). LY294002 treatment did not cause dephosphorylation of KIT, whereas imatinib mesylate caused AKT dephosphorylation, indicating that KIT is an upstream mediator of PI3K and AKT in GIST. As expected, 1-hour treatment caused dephosphorylation of KIT and AKT (Fig. 3*A* and *B, lane IM*), and 1-hour U0126 (Fig. 3*A* and *B, lane U*) treatment did not. Finally, LY294002 treatment clearly resulted in decreased glucose uptake in both cell lines as a function of time (Fig. 3*C*). This result suggests that glucose uptake in GIST cells is mediated by the PI3K and presumably the AKT pathway.

Imatinib-induced apoptosis is independent of AKT signaling. To examine the function of AKT activation in GIST, we infected GIST T1 cells with lentiviral vectors expressing either myristylated AKT1 or myristoylated AKT2 (hereafter referred to as GIST T1/AKT1 and GIST T1/AKT2, respectively), the membrane-bound AKT isoforms that are constitutively active, and the *LacZ* gene as control (hereafter referred to as GIST T1/Lac). The rationale for introducing myristylated AKT isoforms into GIST T1 cells is to determine whether expression of constitutively activated AKT will reverse imatinib mesylate–mediated apoptosis in GIST T1 cells as one might predict based on previous studies. As shown in Fig. 4*A*, imatinib mesylate treatment caused dephosphorylation of KIT as early as 1 hour in all three cell lines, consistent with the result from parental GIST T1 cells (Fig. 2*A*). However, AKT1 and AKT2 remained phosphorylated in GIST T1/AKT1 and GIST T1/AKT2 cells but not in GIST T1/Lac cells. Glycogen synthase kinase-3β (GSK3β), one of the downstream targets for activated AKT, remained phosphorylated in GIST T1/AKT1 and GIST T1/AKT2 cells throughout the treatment. We also evaluated another AKT target, BAD. BAD is a proapoptotic member of the BCL-2 family. AKT has been shown to promote cell survival via its ability to

phosphorylate BAD at Ser^{136} (40, 41). As observed for GSK3β, BAD remained phosphorylated in T1/ATK1 and GIST T1/AKT2 cells treated with imatinib mesylate and LY294002. These results provide additional evidence that the AKT pathway is constitutively active in the AKT1- or AKT2-transduced cells. As expected, U0126 (Fig. 4*A, lane U*) had no effect on KIT, AKT, GKS3β, or BAD phosphorylation.

We then assayed the role of AKT signaling in the growth response to imatinib mesylate. We expected that GIST T1/AKT1 and GIST T1/AKT2 cells would be resistant to imatinib mesylate–induced apoptosis, as AKT is involved in the survival pathway. Surprisingly, imatinib mesylate treatment resulted in cell death even in the presence of constitutively activated AKTs (Fig. 4*B, bottom*). Similarly, parental GIST T1 and GIST T1/Lac cells were also sensitive to imatinib mesylate–induced cell death (Fig. 4*B, top*). The cell death is via an apoptotic pathway as determined by Annexin V staining (data not shown), and phosphorylation of BAD by constitutively active AKT did not prevent cells from undergoing imatinib-induced apoptosis (Fig. 4*A* and *B*). These results show for the first time that although AKT is involved in the survival pathway in many tumors, constitutive expression of myristoylated AKT1 or ATK2 fails to rescue imatinib mesylate–induced growth suppression and apoptosis in GIST cells.

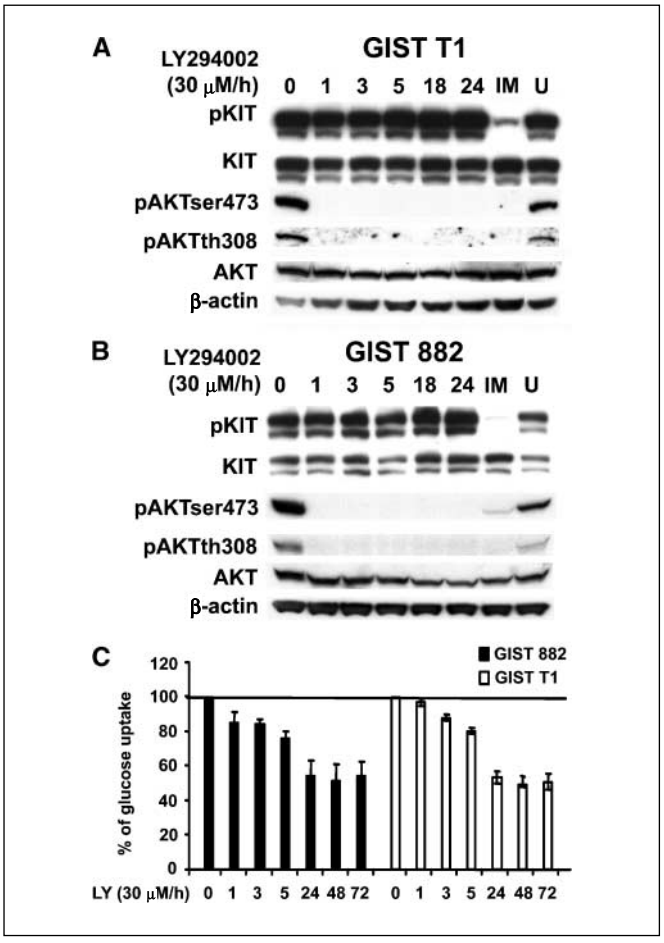

Figure 3. LY294002 treatment of GIST cells. GIST T1 (*A*) and GIST 882 (*B*) cells were treated with LY294002 for the indicated time points. Equal amounts of whole-cell extract from each sample were subjected to immunoblotting using specific antibodies as indicated. *Lanes IM* and *U,* cells were treated with 10 μmol/L imatinib mesylate and 10 μmol/L U0126, respectively. *C,* glucose uptake assays of GIST 882 and GIST T1 cells treated with LY294002 (*LY*) for the indicated time points. The percentage of uptake was normalized to nontreated samples (0 hour). *Columns,* statistical summary of four independent experiments.

We next tested if glucose uptake was dependent on AKT signaling in GISTs. We showed that glucose uptake in GIST cells is dependent on both AKT1 and AKT2 isoforms (Fig. 4*C*). The PI3K-AKT pathway is the major mediator for glucose transport via the insulin receptor pathway in insulin-responsive cells. Here, we show that, in the absence of insulin stimulation, GIST cells expressing constitutively active AKT1 or AKT2 are able to maintain high levels of glucose uptake even when KIT activation is inhibited by imatinib mesylate. This result indicates that glucose uptake in GIST is AKT dependent, in contrast to imatinib mesylate–induced effects on cell growth and apoptosis, which can be AKT independent.

PI3K mediates the therapeutic effects of imatinib independent of AKT. KIT phosphorylation at the Tyr^{719} leads to the activation of PI3K (13). Mutation of this residue completely disrupts PI3K binding to KIT and reduces PI3K-dependent AKT activation by 90% (12). To establish whether PI3K activity has an essential role in KIT signaling and whether it is essential for imatinib mesylate–mediated effects on GIST cell growth and apoptosis, we again examined the inhibitory effect of LY294002. In GIST T1/AKT1 cells, it was very clear that LY294002 had no inhibitory effect on myristoylated AKT1 at both Ser^{473} and Thr^{308} residues (Fig. 5*A, middle*) but inhibited the endogenous levels of phosphorylated AKT at these two residues (Fig. 5*A, arrowheads*). The doublet bands of phosphorylated AKT represent the myristoylated AKT1 and endogenous AKT (Fig. 5*A, arrowheads*). Likewise, LY294002 did not inhibit myristoylated AKT2 phosphorylation in GIST T1/AKT2 cells (Fig. 5*A, right*). In addition, GSK3β and BAD also remain phosphorylated throughout treatment due to constitutively active AKT1 or AKT2 (Fig. 5*A* and *B*). As expected, LY294002 strongly inhibits phosphorylation of endogenous AKT in GIST T1/Lac cells (Fig. 5*A, left*). These results confirm that myristoylated AKT isoforms remain phosphorylated in transduced cells even with LY294002 treatment.

Similar to the imatinib mesylate–induced apoptosis (Fig. 4*B*), we noted that GIST T1/AKT1 and GIST T1/AKT2 cells also display LY294002-induced growth arrest. We determined that the IC_{50} for LY294002 of GIST T1 cells is 5 μmol/L (data not shown). Additionally, parental T1 and GIST T1/Lac, when treated with LY294002, showed similar degrees of arrest due to PI3K inhibition as well as decreased levels of phosphorylation of AKT at Ser^{473} by immunoblots (Fig. 5*C, top, insets*). It is then surprising that LY294002 also caused cell arrest in GIST T1/AKT1 and GIST T1/AKT2 cells despite there being no inhibition of phosphorylation of AKT (Fig. 5*C, bottom, insets*). However, these results are consistent with the studies of imatinib mesylate, suggesting that PI3K inhibition, independent of AKT inhibition, may help mediate the effects of KIT inhibition by imatinib mesylate.

Next, we examined whether PI3K signaling was involved in glucose uptake in GIST cells. Unlike imatinib mesylate, LY294002 preferentially inhibits glucose uptake in myristoylated AKT1 cells better than in myristoylated AKT2 cells. The rate of glucose uptake remained high throughout treatment in GIST T1/AKT2 cells. However, glucose uptake in GIST T1/Lac and GIST T1/AKT1 cells was inhibited by LY294002 (Fig. 5*D*). This result suggests that the AKT2 isoform may have a dominant role in glucose uptake in GIST.

Mechanistic evaluation of imatinib mesylate on the glucose transporter Glut4. Finally, we examined the mechanism that regulates glucose transport in GIST cells. We focused our studies

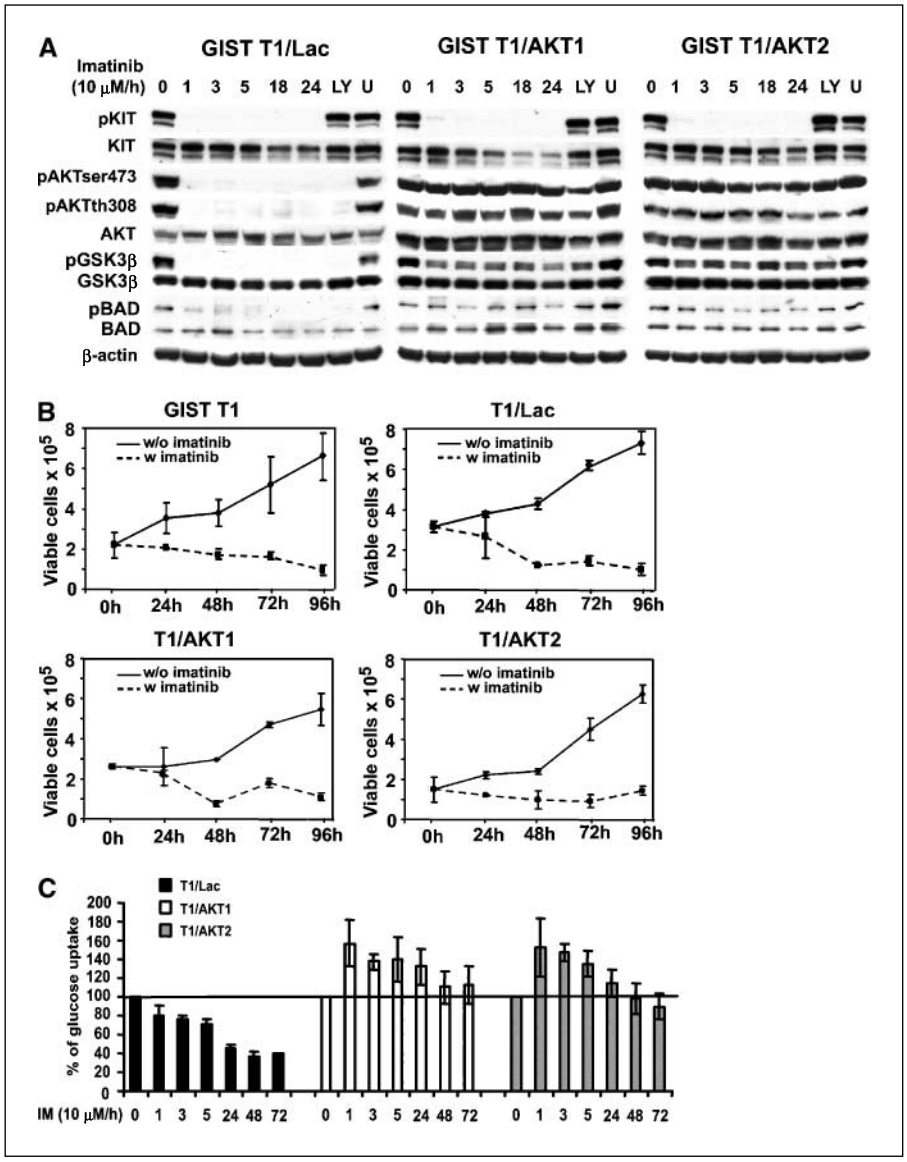

Figure 4. Imatinib-induced apoptosis is independent of AKT signaling and glucose uptake. *A,* GIST T1/Lac, GIST T1/AKT1, and GIST T1/AKT2 cells were treated with 10 μmol/L imatinib mesylate for the indicated time points. Equal amounts of whole-cell extract from each sample were subjected to immunoblotting using specific antibodies as indicated. *Lanes LY* and *U,* cells were treated with 30 μmol/L LY294002 and 10 μmol/L U0126, respectively. *B,* viability assays. Cells were treated with 1 μmol/L imatinib mesylate, and total viable cells were measured as described in Materials and Method at the indicated time points. *C,* glucose uptake assays. Cells were treated with imatinib mesylate (*IM*) for the indicated time points. Percentage of uptake was normalized to nontreated samples (0 hour). *Columns,* statistical summary of four independent experiments.

on the expression and localization of two prominent glucose transporters, Glut1 and Glut4. Parental GIST 882 and GIST T1, GIST T1/Lac, GIST T1/AKT1, and GIST T1/AKT2 cells were treated with imatinib mesylate for 48 hours followed by immunoblot assays of the plasma membrane fraction (Fig. 6*A* and *B*). Densitometry scanning showed that, in GIST 882, GIST T1, and GIST T1/Lac cells, the amount of Glut4 transporter on the plasma membrane fraction was reduced in imatinib mesylate–treated cells compared with nontreated cells (see relative plasma membrane level, Fig. 6*A*). The reduction of the plasma membrane-bound Glut4 by imatinib mesylate leads to decreased glucose uptake (Figs. 2*C* and 4*C*). Treatment with imatinib mesylate caused Glut4 to translocate, via endocytosis, from the plasma membrane to the cytosol as evidenced by lower levels of plasma membrane-bound Glut4. By contrast, GIST T1/AKT1 and GIST T1/AKT2 cells have comparable amounts of plasma membrane-bound Glut4 that was not reduced by imatinib mesylate treatment. Na/K ATPase-α1 antibody was used as a plasma membrane marker and a loading control. The relative level of plasma membrane-bound Glut4 for each sample was derived by normalizing Glut4 intensity with Na/K ATPase-α1 intensity. For purity control, we also blotted the membrane with β-actin, the marker for cytosolic compartment (data not shown). We have shown that Glut1 is also expressed in GIST cells, with the majority sequestered in cytosolic membrane vesicles (data not shown).

We further confirmed the imatinib mesylate induced Glut4 translocation by immunofluorescent staining. GIST 882 and GIST T1 cells without imatinib mesylate displayed staining of the plasma membrane as well as intracellular microsomes of membrane-bound Glut4 (Fig. 6*C, 1-3* and *7-9*), whereas imatinib mesylate–treated cells had prominent cytosolic staining of intracellular microsomes (Fig. 6*C, 4-6* and *10-12*). The prominent staining of intracellular microsomes in imatinib mesylate–treated cells could be due to endocytosis of Glut4 from plasma membrane or sequestering of intracellular microsomes from exocytosis. In combination with our data above, our results suggest that imatinib mesylate increases Glut4 endocytosis, resulting in decreased plasma membrane-bound Glut4 molecules and leading to reduction of

glucose transport into cells. Likewise, GIST T1/Lac cells also display imatinib mesylate–mediated decrease of plasma membrane-bound Glut4. However, expression of constitutively active AKT1 or AKT2 did not result in imatinib mesylate–induced endocytosis of Glut4 (see Supplementary Data). These results agree with the glucose uptake assays shown in Figs. 4 and 5.

Discussion

The findings presented here show a novel insight into the molecular exploration of the therapeutic effects of imatinib mesylate in the treatment of GIST cells specifically with regard to drug-induced tumor cell killing. Imatinib mesylate leads to the reduction of glucose uptake in GIST cells in an AKT-dependent manner and inhibition of cell growth and induction of apoptosis in an AKT-independent manner. Importantly, we have shown that reduction of glucose uptake, which is quantified by FDG-PET and is prognostic of tumor response to imatinib mesylate, may not absolutely correlate with decreased cell growth and tumor shrinkage via apoptosis. Initially, we established that GIST cell lines harboring mutations in c-*KIT* display differential sensitivity to imatinib mesylate and that inhibition of KIT phosphorylation

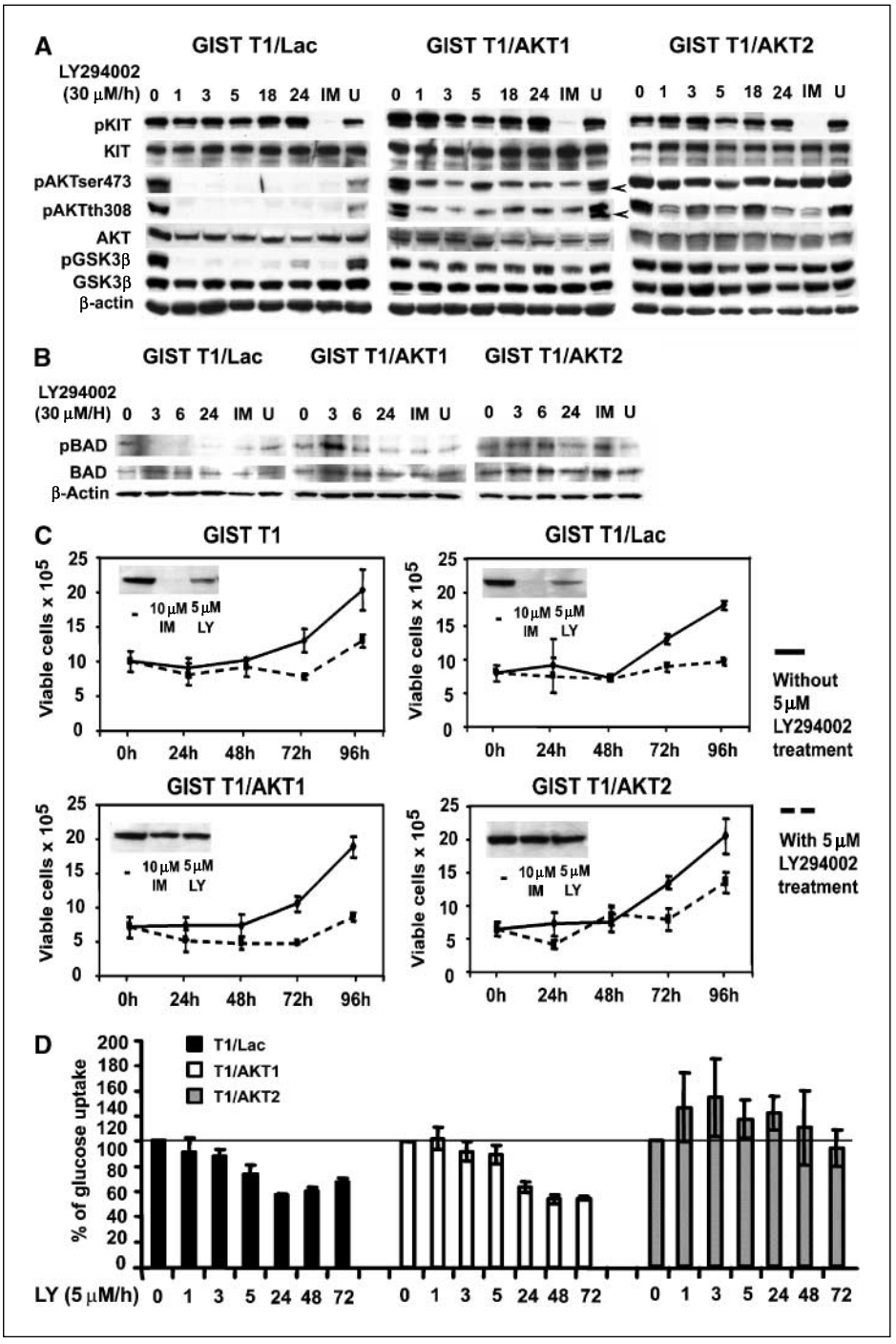

Figure 5. LY294002 treatment of GIST T1 cells expressing constitutive active AKT1 or AKT2. *A* and *B,* GIST T1/Lac, GIST T1/AKT1, and GIST T1/AKT2 cells were treated with LY294002 for the indicated time points. Equal amounts of whole-cell extract from each sample were subjected to immunoblotting using specific antibodies as indicated. *Lanes IM* and *U,* cells were treated with 10 μmol/L imatinib mesylate and 10 μmol/L U0126, respectively. *C,* viability assays. Cells were treated with imatinib mesylate, and total viable cells were measured at the indicated time points. *Insets,* immunoblots for phosphorylated AKT Ser^{473}. *D,* glucose uptake assays. Cells were treated with LY294002 for the indicated time points. Percentage of uptake was normalized to nontreated samples (0 hour). *Columns,* statistical summary of three independent experiments.

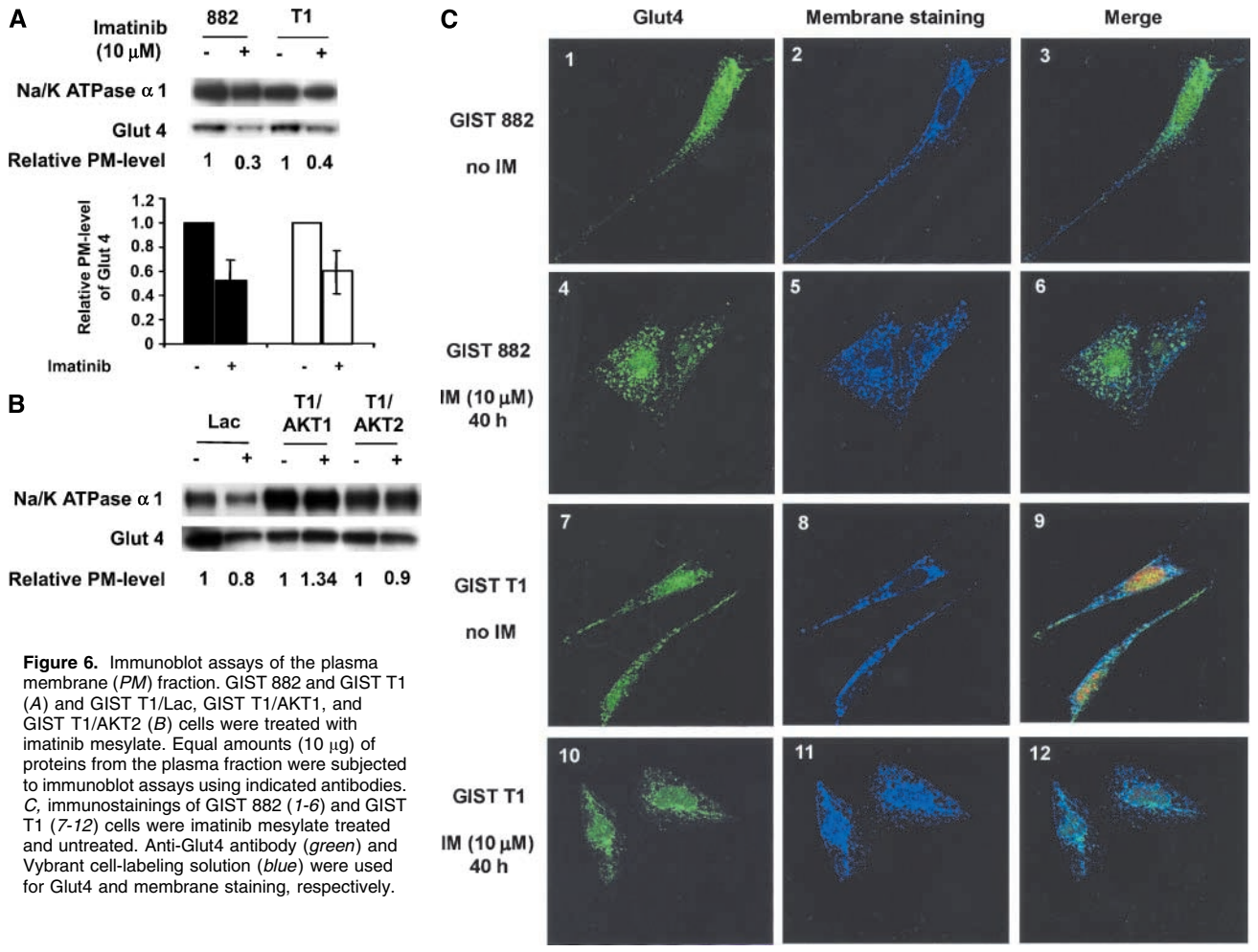

Figure 6. Immunoblot assays of the plasma membrane (*PM*) fraction. GIST 882 and GIST T1 (*A*) and GIST T1/Lac, GIST T1/AKT1, and GIST T1/AKT2 (*B*) cells were treated with imatinib mesylate. Equal amounts (10 μg) of proteins from the plasma fraction were subjected to immunoblot assays using indicated antibodies. *C,* immunostainings of GIST 882 (*1-6*) and GIST T1 (*7-12*) cells were imatinib mesylate treated and untreated. Anti-Glut4 antibody (*green*) and Vybrant cell-labeling solution (*blue*) were used for Glut4 and membrane staining, respectively.

is not the sole predictor of the biological response. These results are consistent with clinical trial results of imatinib mesylate, which found that GIST tumors with KIT mutations in exon 11 (e.g., GIST T1) have the highest response rate and disease-free survival compared with mutations outside this region (e.g., GIST 882; ref. 36). In our current study, we have shown that both GIST cell lines undergo imatinib mesylate–mediated inhibition of KIT autophosphorylation and growth arrest but that drug treatment of GIST T1 cells elicits a more efficient apoptotic response.

It was suggested in a recent report that imatinib mesylate caused a decrease in glucose uptake and that this enhanced the cytotoxic effect of imatinib mesylate only in an imatinib mesylate–sensitive tumor. An imatinib mesylate–resistant tumor showed no changes in FDG uptake (42). That report agrees with conventional observations, that is, a decrease in glucose uptake by tumor is a direct reflection of the therapeutic effect of drug treatment. However, that study used KIT-transfected myeloid progenitor cells as a GIST model, which may not accurately mimic *de novo* response of GIST. In our study, we examined whether imatinib mesylate has influence on glucose uptake by GIST cells and the association of this glucose uptake with analytic measurement of GIST cell survival. We have shown that imatinib mesylate directly decreases glucose uptake, in an AKT-dependent manner, in both GIST cell lines despite the fact that one cell line is sensitive and the other is resistant to imatinib mesylate–mediated apoptosis. Furthermore, constitutively active AKT1 or AKT2 isoforms did not rescue GIST T1 cells from imatinib mesylate–induced apoptosis, suggesting that AKT activation may not be the sole mechanism for GIST cell survival after addition of imatinib mesylate. However, a separate AKT-mediated mechanism is responsible for glucose uptake in GIST cells as shown by constitutively active AKT1 or AKT2 isoforms capable of reversing the inhibitory effect of imatinib mesylate on glucose uptake. Collectively, our results show that, when treated with imatinib mesylate, the cell growth and glucose uptake in GIST are two mutually exclusive events, with AKT-independent cell growth and survival and AKT-dependent glucose uptake. Most importantly, we have shown that the therapeutic effect of imatinib mesylate in GIST may be independent of AKT despite glucose uptake being dependent on AKT. These results suggest that loss of FDG uptake as detected on PET scan may be a surrogate for but not pathognomic of the actual tumor cell killing.

In addition, we show *in vitro* that gain-of-function mutations in KIT lead to constitutive activation and result in increased glucose transport in GIST cells in an insulin-independent manner (data not shown). The high rate of glucose uptake in GIST is

therefore a biological phenomena regulated by the constitutively active KIT/PI3K/AKT pathway, which maximizes AKT activity. These results indicate that the high rate of glucose uptake in GIST tumor cells may correlate closely with AKT-dependent tumor survival mechanisms.

Finally, we have shown a mechanism that mediates glucose transport in GIST. We show that the glucose transporter Glut4 and, to a lesser extent, Glut1 are prominent on the plasma membrane of GIST 882 and GIST T1 cells (Fig. 6; data not shown). It has been shown previously that Glut4 transporter mediates the entry of glucose into certain tissues (43, 44), and Glut4 expression has been found in breast, gastric, and other malignancies (45–51). In our study, we show that the expression of Glut4 in GIST cells is located in both plasma membrane and cytoplasmic compartments. However, on imatinib mesylate treatment, there is a significant decrease of membrane-bound Glut4 molecules in GIST 882 and GIST T1 cells, indicating that the endocytosis pathway of Glut4 is activated after imatinib mesylate treatment of GIST cells. Overall, these collective findings contribute to a clearer understanding of the molecular mechanisms involved in the therapeutic benefit of imatinib mesylate in GIST.

Acknowledgments

Received 11/1/2005; revised 2/22/2006; accepted 3/10/2006.

Grant support: NIH grant CA106588-01, a supplement to grant 3 U10 CA21661-27, and Ovarian Cancer Specialized Program of Research Excellence grant P50 CA83638, by an appropriation from the Commonwealth of Pennsylvania (A.K. Godwin); National Research Service Award Postdoctoral Fellowship (C. Tarn); and the Pennsylvania Department of Health.

The costs of publication of this article were defrayed in part by the payment of page charges. This article must therefore be hereby marked *advertisement* in accordance with 18 U.S.C. Section 1734 solely to indicate this fact.

We thank Dr. Morris Birnbaum for generously providing anti-Glut4 antibody, the Image Core Facility (Fox Chase Cancer Center) for image processing and analyzing, the Biosample Repository and Tumor Bank Core Facilities (Fox Chase Cancer Center) for specimens, Tania Stutman, and the GIST Cancer Research Fund.

References

1. Perez-Atayde AR, Shamberger RC, Kozakewich HW. Neuroectodermal differentiation of the gastrointestinal tumors in the Carney triad. An ultrastructural and immunohistochemical study. Am J Surg Pathol 1993;17:706–14.
2. Sircar K, Hewlett BR, Huizinga JD, Chorneyko K, Berezin I, Riddell RH. Interstitial cells of Cajal as precursors of gastrointestinal stromal tumors. Am J Surg Pathol 1999;23:377–89.
3. Kindblom LG, Remotti HE, Aldenborg F, Meis-Kindblom JM. Gastrointestinal pacemaker cell tumor (GIPACT): gastrointestinal stromal tumors show phenotypic characteristics of the interstitial cells of Cajal. Am J Pathol 1998;152:1259–69.
4. Hirota S, Isozaki K, Moriyama Y, et al. Gain-of-function mutations of c-kit in human gastrointestinal stromal tumors. Science 1998;279:577–80.
5. Ricotti E, Fagioli F, Garelli E, et al. c-kit is expressed in soft tissue sarcoma of neuroectodermic origin and its ligand prevents apoptosis of neoplastic cells. Blood 1998;91:2397–405.
6. Heinrich MC, Corless CL, Duensing A, et al. PDGFRA activating mutations in gastrointestinal stromal tumors. Science 2003;299:708–10.
7. Claesson-Welsh L, Eriksson A, Westermark B, Heldin CH. cDNA cloning and expression of the human A-type platelet-derived growth factor (PDGF) receptor establishes structural similarity to the B-type PDGF receptor. Proc Natl Acad Sci U S A 1989;86:4917–21.
8. Yarden Y, Escobedo JA, Kuang WJ, et al. Structure of the receptor for platelet-derived growth factor helps define a family of closely related growth factor receptors. Nature 1986;323:226–32.
9. Coussens L, Van Beveren C, Smith D, et al. Structural alteration of viral homologue of receptor proto-oncogene fms at carboxyl terminus. Nature 1986;320:277–80.
10. Rosnet O, Schiff C, Pebusque MJ, et al. Human FLT3/FLK2 gene: cDNA cloning and expression in hematopoietic cells. Blood 1993;82:1110–9.
11. Rousset D, Agnes F, Lachaume P, Andre C, Galibert F. Molecular evolution of the genes encoding receptor tyrosine kinase with immunoglobulinlike domains. J Mol Evol 1995;41:421–9.
12. Blume-Jensen P, Jiang G, Hyman R, Lee KF, O'Gorman S, Hunter T. Kit/stem cell factor receptor-induced activation of phosphatidylinositol 3′-kinase is essential for male fertility. Nat Genet 2000;24:157–62.
13. Sattler M, Salgia R, Shrikhande G, et al. Steel factor induces tyrosine phosphorylation of CRKL and binding of CRKL to a complex containing c-kit, phosphatidylinositol 3-kinase, and p120(CBL). J Biol Chem 1997;272:10248–53.
14. Kabarowski JH, Allen PB, Wiedemann LM. A temperature sensitive p210 BCR-ABL mutant defines the primary consequences of BCR-ABL tyrosine kinase expression in growth factor dependent cells. EMBO J 1994;13:5887–95.
15. Lopez-Ilasaca M, Li W, Uren A, et al. Requirement of phosphatidylinositol-3 kinase for activation of JNK/SAPKs by PDGF. Biochem Biophys Res Commun 1997;232:273–7.
16. Shen Y, Devgan G, Darnell JE, Jr., Bromberg JF. Constitutively activated Stat3 protects fibroblasts from serum withdrawal and UV-induced apoptosis and antagonizes the proapoptotic effects of activated Stat1. Proc Natl Acad Sci U S A 2001;98:1543–8.
17. Atfi A, Prunier C, Mazars A, et al. The oncogenic TEL/PDGFR β fusion protein induces cell death through JNK/SAPK pathway. Oncogene 1999;18:3878–85.
18. Miettinen M, Paal E, Lasota J, Sobin LH. Gastrointestinal glomus tumors: a clinicopathologic, immunohistochemical, and molecular genetic study of 32 cases. Am J Surg Pathol 2002;26:301–11.
19. van Oosterom AT, Judson IR, Verweij J, et al. Update of phase I study of imatinib (STI571) in advanced soft tissue sarcomas and gastrointestinal stromal tumors: a report of the EORTC Soft Tissue and Bone Sarcoma Group. Eur J Cancer 2002;38 Suppl 5:S83–7.
20. Demetri GD. Identification and treatment of chemoresistant inoperable or metastatic GIST: experience with the selective tyrosine kinase inhibitor imatinib mesylate (STI571). Eur J Cancer 2002;38 Suppl 5:S52–9.
21. Druker BJ, Tamura S, Buchdunger E, et al. Effects of a selective inhibitor of the Abl tyrosine kinase on the growth of Bcr-Abl positive cells. Nat Med 1996;2:561–6.
22. Buchdunger E, Cioffi CL, Law N, et al. Abl protein-tyrosine kinase inhibitor STI571 inhibits *in vitro* signal transduction mediated by c-kit and platelet-derived growth factor receptors. J Pharmacol Exp Ther 2000;295:139–45.
23. Li P, Wei J, West AB, Perle M, Greco MA, Yang GC. Epithelioid gastrointestinal stromal tumor of the stomach with liver metastases in a 12-year-old girl: aspiration cytology and molecular study. Pediatr Dev Pathol 2002;5:386–94.
24. Frolov A, Chahwan S, Ochs M, et al. Response markers and the molecular mechanisms of action of Gleevec in gastrointestinal stromal tumors. Mol Cancer Ther 2003;2:699–709.
25. Joensuu H, Roberts PJ, Sarlomo-Rikala M, et al. Effect of the tyrosine kinase inhibitor STI571 in a patient with a metastatic gastrointestinal stromal tumor. N Engl J Med 2001;344:1052–6.
26. Demetri GD, von Mehren M, Blanke CD, et al. Efficacy and safety of imatinib mesylate in advanced gastrointestinal stromal tumors. N Engl J Med 2002;347:472–80.
27. van Oosterom AT, Judson I, Verweij J, et al. Safety and efficacy of imatinib (STI571) in metastatic gastrointestinal stromal tumours: a phase I study. Lancet 2001;358:1421–3.
28. Warburg O. On the origin of cancer cells. Science 1956;123:309–14.
29. Flier JS, Mueckler MM, Usher P, Lodish HF. Elevated levels of glucose transport and transporter messenger RNA are induced by ras or src oncogenes. Science 1987;235:1492–5.
30. Semenza GL, Wang GL. A nuclear factor induced by hypoxia via *de novo* protein synthesis binds to the human erythropoietin gene enhancer at a site required for transcriptional activation. Mol Cell Biol 1992;12:5447–54.
31. Verweij J, van Oosterom A, Blay JY, et al. Imatinib mesylate (STI-571 Glivec, Gleevec) is an active agent for gastrointestinal stromal tumours, but does not yield responses in other soft-tissue sarcomas that are unselected for a molecular target. Results from an EORTC Soft Tissue and Bone Sarcoma Group phase II study. Eur J Cancer 2003;39:2006–11.
32. Druker BJ, Sawyers CL, Kantarjian H, et al. Activity of a specific inhibitor of the BCR-ABL tyrosine kinase in the blast crisis of chronic myeloid leukemia and acute lymphoblastic leukemia with the Philadelphia chromosome. N Engl J Med 2001;344:1038–42.
33. Gottschalk S, Anderson N, Hainz C, Eckhardt SG, Serkova NJ. Imatinib (STI571)-mediated changes in glucose metabolism in human leukemia BCR-ABL-positive cells. Clin Cancer Res 2004;10:6661–8.
34. Taguchi T, Sonobe H, Toyonaga S, et al. Conventional and molecular cytogenetic characterization of a new human cell line, GIST-T1, established from gastrointestinal stromal tumor. Lab Invest 2002;82:663–5.
35. Cross FR, Garber EA, Pellman D, Hanafusa H. A short sequence in the p60src N terminus is required for p60src myristylation and membrane association and for cell transformation. Mol Cell Biol 1984;4:1834–42.
36. Heinrich MC, Corless CL, Demetri GD, et al. Kinase mutations and imatinib response in patients with metastatic gastrointestinal stromal tumor. J Clin Oncol 2003;21:4342–9.
37. Lux ML, Rubin BP, Biase TL, et al. KIT extracellular and kinase domain mutations in gastrointestinal stromal tumors. Am J Pathol 2000;156:791–5.
38. Takahashi Y, Noguchi T, Takeno S, Uchida Y, Shimoda H, Yokoyama S. Gastrointestinal stromal tumor of the duodenal ampulla: report of a case. Surg Today 2001;31:722–6.
39. Stroobants S, Goeminne J, Seegers M, et al. 18FDG-Positron emission tomography for the early prediction of response in advanced soft tissue sarcoma treated with imatinib mesylate (Glivec). Eur J Cancer 2003;39:2012–20.

40. del Peso L, Gonzalez-Garcia M, Page C, Herrera R, Nunez G. Interleukin-3-induced phosphorylation of BAD through the protein kinase Akt. Science 1997;278:687–9.
41. Zha J, Harada H, Yang E, Jockel J, Korsmeyer SJ. Serine phosphorylation of death agonist BAD in response to survival factor results in binding to 14-3-3 not BCL-X(L). Cell 1996;87:619–28.
42. Cullinane C, Dorow DS, Kansara M, et al. An *in vivo* tumor model exploiting metabolic response as a biomarker for targeted drug development. Cancer Res 2005;65:9633–6.
43. Silverman M. Structure and function of hexose transporters. Annu Rev Biochem 1991;60:757–94.
44. Thorens B, Charron MJ, Lodish HF. Molecular physiology of glucose transporters. Diabetes Care 1990; 13:209–18.
45. Nagamatsu S, Sawa H, Wakizaka A, Hoshino T. Expression of facilitative glucose transporter isoforms in human brain tumors. J Neurochem 1993;61:2048–53.
46. Chiaramonte R, Bartolini E, Testolin C, Comi P. Regulation of the human glut4 gene expression in tumor RD18 cell line. Pathobiology 1998;66:191–5.
47. Mioni R, Chiarelli S, Xamin N, et al. Evidence for the presence of glucose transporter 4 in the endometrium and its regulation in polycystic ovary syndrome patients. J Clin Endocrinol Metab 2004;89:4089–96.
48. Moadel RM, Weldon RH, Katz EB, et al. Positherapy: targeted nuclear therapy of breast cancer with 18F-2-deoxy-2-fluoro-D-glucose. Cancer Res 2005;65:698–702.
49. Binder C, Binder L, Marx D, Schauer A, Hiddemann W. Deregulated simultaneous expression of multiple glucose transporter isoforms in malignant cells and tissues. Anticancer Res 1997;17:4299–304.
50. Noguchi Y, Marat D, Saito A, et al. Expression of facilitative glucose transporters in gastric tumors. Hepatogastroenterology 1999;46:2683–9.
51. Noguchi Y, Sato S, Marat D, et al. Glucose uptake in the human gastric cancer cell line, MKN28, is increased by insulin stimulation. Cancer Lett 1999;140:69–74.